Identification of the SiF_6^{2-} dianion by accelerator mass spectrometry and a fully relativistic computation of its photodetachment spectrum

Hubert Gnaser,[1,*] Robin Golser,[2] Markus Pernpointner,[3] Oliver Forstner,[2] Walter Kutschera,[2] Alfred Priller,[2] Peter Steier,[2] and Anton Wallner[2]

[1]*Fachbereich Physik, Technische Universität Kaiserslautern, D-67663 Kaiserslautern, Germany*

[2]*Vienna Environmental Research Accelerator, Fakultät für Physik, Universität Wien, A-1090 Wien, Austria*

[3]*Theoretische Chemie, Universität Heidelberg, Im Neuenheimer Feld 229, D-69120 Heidelberg, Germany*

(Received 19 March 2008; published 23 May 2008)

The small doubly-charged molecular anion SiF_6^{2-} was studied by two distinct approaches, one experimental the other theoretical. The dianion was produced in the gas phase by sputtering a Li_2SiF_6 specimen with Cs^+ ions and was detected by means of accelerator mass spectrometry. The identification was via the $^{29}Si^{19}F_6^{2-}$ isotopomer; it has an odd total mass and therefore the dianion shows up at a half-integral mass-to-charge ratio (M/q=71.5 amu) in the mass spectrum, facilitating a positive identification. The flight time through the mass spectrometer of $\approx$10 μs establishes a lower limit with respect to the intrinsic lifetime of this species. Attempts to detect the SiF_6^{2-} dianion also by secondary-ion mass spectrometry failed, but provided an upper limit in terms of its formation probability with respect to the F^- ion of $^{29}Si^{19}F_6^{2-}/^{19}F^- < 2\times10^{-9}$. Furthermore, theoretical calculations of the photoelectron spectrum by means of the relativistic one-particle propagator predict considerable stability of the dianion against autodetachment. The first ionization potential of SiF_6^{2-} was determined as 2.79 eV at the optimized bond length of 1.718 Å in the gas phase.

DOI: 10.1103/PhysRevA.77.053203 PACS number(s): 36.40.−c, 79.20.Rf, 33.15.Ta, 82.80.Ms

I. INTRODUCTION

The existence of doubly-charged negative ions or, more generally, of multiply charged anions (MCAs) in the gas phase has attracted considerable theoretical and experimental attention [1–7]. While small dianions and trianions (such as O^{2-}, CO_3^{2-}, SO_4^{2-}, or PO_4^{3-}) are ubiquitous in solutions and in the solid state, the stability of MCAs in the gas phase may be limited by the Coulombic repulsion of the excess electrons that strongly favors the emission of one electron and supports the dissociation of the molecular framework into two monoanionic fragments [6]. From a theoretical point of view, a stable gas-phase MCA must possess two basic properties: First, it must be stable with respect to electron autodetachment, and second, it must be stable with respect to fragmentation of the nuclear framework.

The first clear experimental observation, by Schauer, Williams, and Compton [8], of *small, long-lived* dianionic species in the gas phase reported the generation of C_n^{2-} (n=7–28) by sputtering and their detection by mass spectrometry, implying lifetimes of at least some 10^{-5} s. The existence of these dianions was later confirmed and studied in some detail by other groups [9–11] and triggered a search for other dianions and MCAs by experimental and theoretical means (see, e.g., [2,6,12] for reviews).

The aim of the present work is to report the experimental detection of a dianion, SiF_6^{2-}, produced by sputtering and monitored by means of accelerator mass spectrometry. In addition, the SiF_6^{2-} dianion is theoretically characterized by the computation of its relativistic photoelectron (PE) spectrum. PE spectra provide valuable information about the electronic structure and bonding in a specific system and their accurate prediction by *ab initio* methods still is a challenging task. Especially for the understanding of the unusual electronic structure of multiply charged anions (MCAs) in the gas phase, PE spectra are an indispensable tool [1–3,6,13–19]. In MCAs there is a strong Coulombic repulsion of the excess electrons causing a repulsive Coulomb barrier (RCB) that leads to a metastable state with respect to autodetachment of the MCA into a free electron and a negatively charged ion [5,20]. These intrinsic properties of MCAs can well be analyzed by PE spectroscopy and a growing number of accessible gas phase MCAs allows for direct comparison of experimental and theoretical results (see [6] for a review until the year 2002).

Several fluorine-carrying dianions have been observed in experiments using sputtering for their formation such as BeF_4^{2-}, MgF_4^{2-} [21], CaF_4^{2-} [22], HfF_6^{2-} [23], ZrF_6^{2-} [24], and LiF_3^{2-} [25,26]. It is noted that two of them, ZrF_6^{2-} and HfF_6^{2-}, are similar to SiF_6^{2-} in that, similar to Si, also Zr and Hf have four valence electrons. Theoretical investigations identified a number of small stable F-containing dianions such as MX_3^{2-} (M=Li, Na, K; X=F, Cl) [27–30], MX_4^{2-} (M=Be, Mg, Ca; X=F, Cl) [31,32], and PtX_6^{2-} (X=*F*, Cl, Br) [33,34].

An efficient *ab initio* approach to theoretical PE spectra is the one-particle propagator (Green's function) method which was followed in this work. The sought spectral information is hereby contained in the eigenvalues (poles) and eigenvectors (residues) of the propagator expression where the algebraic diagrammatic construction (ADC) scheme [35] was applied for its computation. Large relativistic effects are not to be expected in silicon-containing compounds but a unified and consistent treatment of relativity and electron correlation is mandatory for heavier systems (see, for example, [36]). In order to treat the effect of spin-orbit coupling appropriately in our system the relativistic implementation of the propaga-

*Corresponding author, gnaser@rhrk.uni-kl.de

tor, the Dirac-Hartree-Fock (DHF)-ADC(3) method [37,38] was also applied here. The ADC(n) formalism is a size-consistent combination of perturbation theory and matrix diagonalization including diagrams up to the nth order consistently. By application of the DHF-ADC method, errors due to the neglect of spin-orbit splitting and due to the interplay of relativistic effects and electron correlation are avoided completely and small spin-orbit coupling effects will be observable in the SiF_6^{2-} PE spectrum. All relativistic calculations were done with the program package DIRAC04 [39] to which the DHF-ADC(3) code [40] was added.

II. EXPERIMENT

The measurements have been performed at the Vienna Environmental Research Accelerator (VERA), an accelerator mass spectrometer with a terminal voltage of up to 3 MeV (National Electrostatics Corporation). The ion source is optimized for high output and produces Cs^+ currents of the order of 0.5 mA in close vicinity of the samples. The major components of the low-energy side are a 45° spherical electrostatic analyzer and a 90° double-focusing injection magnet. Passing these devices, negative ions are then accelerated in a 3 MV Pelletron tandem accelerator and stripped to positive ions at the terminal stripper operated with Ar or O_2. At the high-energy side, VERA is equipped with a 90° double-focusing analyzing magnet and a 90° spherical electrostatic analyzer with 2.0 m bending radius. For the measurements of dianions, a silicon surface-barrier detector is used. A detailed description of this instrument is given in [41,42].

In addition, experiments were performed in a standard secondary-ion mass spectrometer (SIMS) instrument (Cameca IMS-4f [43]). Primary Cs^+ ions are produced in a surface-ionization source and the ion beam energy is 14.5 keV (beam current ≈100 nA). The sample is at a potential of −4.5 kV and the energy of the emitted negative ions amounts then to $(4.5q)$ keV, with q being the ions' charge state. Mass selection is done in a double-focusing arrangement, consisting of an electrostatic and a magnetic sector field, both with a 90° deflection of the beam; upon passage through the spectrometer, ions are detected by a discrete-dynode electron multiplier. This instrument has been employed in previous studies of dianions [9,11,12,23].

III. COMPUTATIONAL METHODOLOGY

A. The one-particle propagator

The one-particle propagator technique is well established and numerous textbooks [44–46] and review articles [47–55] are dedicated to that formalism. Additionally, a very efficient method for actually solving the Green's function in the framework of perturbation theory consistent up to nth order was developed by Schirmer [35,56] which allows for a straightforward implementation solely based on contractions over totally antisymmetric two-electron integrals and matrix diagonalizations. Due to the combination of algebraic and diagrammatic methods this approach was termed "algebraic diagrammatic construction (ADC)." In the following we restrict ourselves to mentioning the essentials for the relativistic extension of the ADC scheme. In [37,38] it was demonstrated how the non-Dyson version of ADC can be embedded into four-component theory. The contribution of the negative energy states was excluded by application of the "no-pair" formalism derived from QED (see [57] and references therein) but within the diagrammatic framework a perturbational treatment of these contributions would also be possible [58–61]. The starting point is the one-particle Green's function $G_{pq}(t,t')$ (electron propagator) which is defined [44] by the equation

$$G_{pq}(t,t') = -i\langle\Psi_0^N|c_p(t)c_q^\dagger(t')|\Psi_0^N\rangle\Theta(t-t') + i\langle\Psi_0^N|c_q^\dagger(t')c_p(t)|\Psi_0^N\rangle\Theta(t'-t) \quad (1)$$

where $|\Psi_0^N\rangle$ is the *exact* (nondegenerate) ground state of the considered N-particle system, $c_q^\dagger(t)$ $[c_p(t)]$ denote creation (destruction) operators for one-particle states $|\varphi_q\rangle$, and $\Theta(\tau)$ is the Heaviside step function. In the energy representation G_{pq} takes on the form

$$G_{pq}(\omega) = G_{pq}^+(\omega) + G_{pq}^-(\omega) \quad (2)$$

where

$$G_{pq}^+(\omega) = \langle\Psi_0^N|c_p(\omega - \hat{H} + E_0^N + i\eta)^{-1}c_q^\dagger|\Psi_0^N\rangle, \quad (3)$$

$$G_{pq}^-(\omega) = \langle\Psi_0^N|c_q^\dagger(\omega + \hat{H} - E_0^N - i\eta)^{-1}c_p|\Psi_0^N\rangle. \quad (4)$$

Here $\hat{H}$ is the Hamiltonian of the system and E_0^N is the ground-state energy, η is a positive infinitesimal required to define the Fourier transform between the time and energy representation of Eqs. (1) and (2). The parts $\mathbf{G}^+(\omega)$ and $\mathbf{G}^-(\omega)$ contain physical information on the $(N+1)$ and $(N-1)$ particle systems, respectively. This becomes explicit in the spectral representation [44,45], which for the $(N-1)$ particle part reads as

$$G_{pq}^-(\omega) = \sum_n \frac{x_{nq}^* x_{np}}{\omega - \omega_n - i\eta}. \quad (5)$$

Here the pole positions

$$\omega_n = -(E_n^{N-1} - E_0^N) \quad (6)$$

are the (negative) ionization energies of the system, while the residue amplitudes

$$x_{np} = \langle\Psi_n^{N-1}|c_p|\Psi_0^N\rangle \quad (7)$$

are related to spectral intensities. Because we focus on the $(N-1)$ particle system (ionization processes), only the $\mathbf{G}^-(\omega)$ part of the full Green's function is considered further. It should be noted that in the ADC(3) scheme the ionization energies are treated consistently through third order within a $1h$ and $2h1p$ configuration space. Within a wave-function-based approach the same consistency would require a $1h$, $2h1p$, and $3h2p$ configuration space leading to increased computational effort.

The explicit expressions for the DHF-ADC matrix entries consist of functions of the spinor energies ε_r and the relativistic transformed molecular orbital (MO) integrals $V_{pq,rs}$ where the general indices comprise the occupied (hole) and

virtual (particle) spinors in the no pair approximation. In spinor theory no separation of the spatial and spin part is applicable which allows for a direct use of the spin-orbital form of the algebraic expressions derived from the Abrikosov diagrams. For nonrelativistic implementations electron spin is normally integrated out resulting in different sets of working equations for different final state multiplicities. This distinction is unnecessary in DHF-ADC and one obtains all the eigenvalues with one set of equations in a *jj*-coupled framework. Double group and time reversal symmetry are exploited wherever possible. It should be mentioned that all the structural relativistic effects are incorporated in the $V_{pq,rs}$ integrals and ε_r spinor energies simplifying the implementation. The numerical effort for a four-component calculation is higher in the self-consistent field (SCF) and integral transformation step due to the occurrence of the small component basis set and different functions for the $l \pm \frac{1}{2}$ spinor components. However, actual performance runs showed that except from the constant diagrams all ADC matrix block evaluations do not require substantially more computer time than the one-component counterparts once the transformed integrals are available. In the third-order DHF-ADC the so-called constant diagrams are additionally required and calculated by the Dyson expansion method (DEM) [62] which represents the most time-consuming step.

B. Basis sets

Four-component calculations for polyatomic systems are still quite demanding with respect to computational resources and a careful choice of the basis is therefore required. For the silicon and fluorine atoms uncontracted $(16s,10p,3d,2f)$ and $(11s,7p,3d)$ primitive sets were employed ensuring enough diffuseness for the description of the electron ionization. DIRAC04 uses an efficient integral-direct SCF and transformation code eliminating all effects based on basis set contraction. With this basis set a gas-phase structure for the SiF_6^{2-} dianion was optimized at the coupled cluster with single and double excitations (CCSD) level resulting in a Si–F bond length of 1.718 Å always maintaining O_h symmetry. This value is close to a solid-state result of 1.706 Å obtained by Hamilton in the $FeSiF_6 \cdot 6H_2O$ salt [63]. After the SCF step a manifold of occupied and virtual spinors is obtained from which the active space for the electron correlation treatment has to be chosen. In our case the silicon $1s2s2p$ and fluorine $1s$ cores were kept frozen and virtual spinors up to an energy of +2.0 a.u. were included. This value might seem a bit low but had to be chosen in order to keep the active space of tractable size. Nevertheless, the spinor density in the considered energy range is high enough to ensure a proper correlation treatment. The resulting total number of active spinors then amounts to 228 already requiring substantial resources. It was found in numerous calculations that dianions show a pronounced dependence of the first ionization potential on the molecular geometry. Additional high angular momentum functions on silicon and fluorine together with an enlarged correlation space will therefore still alter the obtained results a bit, but exceed our current resources at the moment.

IV. RESULTS AND DISCUSSION

A. The detection of SiF_6^{2-} by mass spectrometry

Dianions are usually formed with low probability in the gas phase. In order to monitor them by mass spectrometry, ion formation and detection has to be maximized. It is well established [64] that Cs^+ bombardment of solids (and the concurrent incorporation of cesium into the near-surface region [65]) causes a prolific generation and emission of *negative* ions from that material. This finding is generally ascribed to a lowering of the sample's work function [66] that, in turn, increases (exponentially) the ionization probability of the sputtered species [64]. This yield enhancement has been shown [67] to be valid also for cluster ions and is of particular importance for the sensitive detection of ions which intrinsically form with low probability such as dianions. Hence, a Cs^+ ion beam is generally utilized for the detection of sputtered anions.

Following the original approach in [8], essentially all experiments carried out to detect doubly-charged negative ions in mass spectrometry, both at low and at high energies, used molecular species with an *odd* total mass M. Dianions are then observed at *half-integral* mass numbers in the spectrum as the electrical and magnetic elements employed always specify the mass-to-charge ratio (M/q). In addition, this provides the possibility to work at low mass resolution and, hence, at a high instrument transmission. While the detection of a mass peak at a *half-integral* mass number is usually a very strong indication for the presence of a dianion in the mass spectrometer, some ambiguities may still arise and this will be discussed below.

As compared to low-energy mass spectrometry, accelerator mass spectrometry (AMS) provides additional means to identify doubly-charged negative molecules. AMS allows to "analyze" a molecular dianion due to the breakup of the molecule into its atomic constituents during the stripping process in a tandem accelerator [10,22,25,26,68]. The experimental scheme is the following: the SiF_6^{2-} dianion, produced by sputtering a Li_2SiF_6 specimen, is detected as $^{29}Si^{19}F_6^{2-}$ at $M/q=71.5$ amu. When negative ions with $M/q=71.5$ amu are injected at the low-energy side of a tandem accelerator (running at 2.7 MV) and the high-energy side is set to detect $^{19}F^{2+}$, up to sixfold coincidences are observed in the energy detector, c.f. Fig. 1. Assuming the negative ions are in fact dianions of mass 143 amu, e.g., $^{29}Si^{19}F_6^{2-}$, such a spectrum can be interpreted as follows: when a particular $^{29}Si^{19}F_6^{2-}$ breaks up in the stripper, each of the atomic constituents ^{29}Si and ^{19}F starts a history of its own. So, after some interactions with the stripper gas, a ^{19}F will exit in charge state 2+ with a certain probability. Since the high-energy side is set to $^{19}F^{2+}$, it will eventually be registered in the energy detector. The total energy measured in the detector depends on the fate of the other ^{19}F from this very dianion. If only one out of the six ^{19}F leaves the stripper in charge state 2+ and comes into the detector, the multichannel analyzer counts it in the peak corresponding to the particle energy, say E_1 (around channel 100 in Fig. 1, labeled $1F$). If two out of the six ^{19}F go into 2+, they may hit the detector simultaneously, yielding $2E_1$ and thus contributing a peak at twice the energy (around

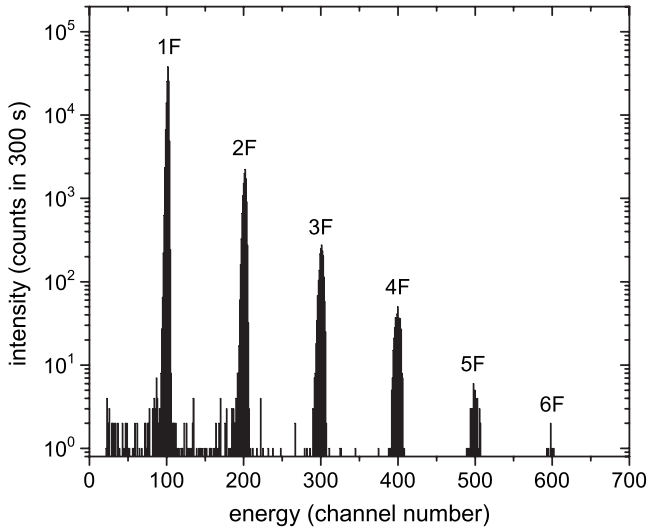

FIG. 1. Energy spectrum measured in a surface barrier detector when negative ions with $M/q=71.5$ amu, i.e., $^{29}Si^{19}F_6^{2-}$, sputtered from a Li_2SiF_6 specimen are injected into the low-energy side of the accelerator and the high-energy side is set to detect $^{19}F^{2+}$.

channel 200 in Fig. 1, labeled $2F$). With a certain probability, even all six ^{19}F from one particular $^{29}Si^{19}F_6^{2-}$ may coincide. It is important to note that the peak-to-peak ratios would not change with source output. This is to be distinguished from pile-up, i.e., the random coincidence of $^{19}F^{2+}$ from different molecules. Indeed, coincidences up to sixfold are observed when ions with $M/q=71.5$ are injected into the accelerator during sputtering of Li_2SiF_6, see Fig. 1. This observation proves that the signal at $M/q=71.5$ contains molecular ions with six ^{19}F atoms, that must be dianions as their masses add up to 114 amu. The remaining mass is then 29 amu which would be ^{29}Si. Varying the M/q value of the injected ions from 71.5 amu to slightly lower or higher values, the sixfold coincidences start to vanish rapidly. Approaching $M/q=71.0$ amu, strong threefold coincidences were observed due to the very abundant $^7Li_2{}^{19}F_3^{2-}$ anion.

Attempts to detect the SiF_6^{2-} dianion also by low-energy mass spectrometry in the SIMS instrument were unsuccessful. As in AMS, the mass spectrometer was set to monitor ions with $M/q=71.5$ amu (corresponding to $^{29}Si^{19}F_6^{2-}$), but no mass peak could be observed. From the background level at $M/q=71.5$ and the intensity of the $^{19}F^-$ ion, an upper limit for the relative formation probability of the dianion, $^{29}Si^{19}F_6^{2-}/{}^{19}F^- < 2\times10^{-9}$ is derived. An estimate based on the AMS signals indicates that this ratio is probably even lower ($<10^{-10}$). Apparently, the higher sensitivity of AMS as compared to the SIMS setup provides the possibility to detect this dianion in the former case, but not in the latter.

The AMS measurements demonstrate clearly that the SiF_6^{2-} dianion is (meta)stable in the gas phase with respect to both electron detachment and fragmentation, on a time scale of at least some 10 μs (the flight time from the ion source to the terminal stripper). The theoretical calculations of the photodetachment spectrum described in the following section, although not directly correlated with the experimental data, substantiate the dianion's stability observed in AMS by determining the electronic structure and the bonding of this dianion.

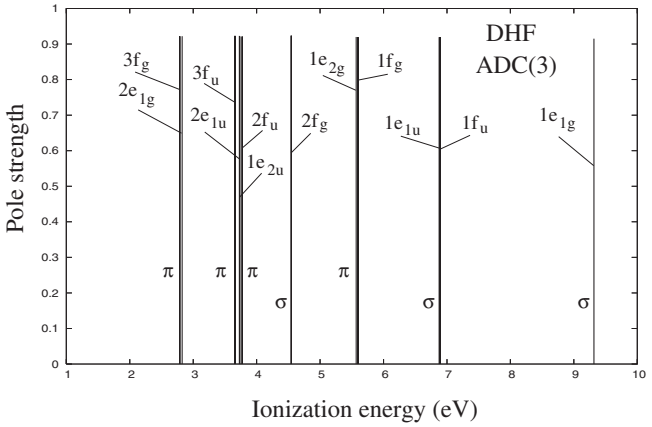

FIG. 2. Computed outer valence DHF-ADC(3) spectrum of SiF_6^{2-} in the range of 0 to 10 eV. The type of bonding (σ or π) is attached to each line with respect to the usual classification.

B. The relativistic SiF_6^{2-} photodetachment spectrum

In Fig. 2 the valence ionization spectrum of the closed shell SiF_6^{2-} dianion is given comprising the space of the ligand-metal σ bonds and the nonbonding ligand π orbitals. The six fluorine p_z orbitals form the σ bonds to the central atom and transform according to the a_{1g}, e_g, and t_{1u} irreducible representations (ireps) in O_h symmetry. The remaining nonbonding fluorine p_x and p_y orbitals form the threefold degenerate t_{1g}, t_{1u}, t_{2g}, and t_{2u} groups each one accommodating six electrons. Since we work in a fully relativistic scheme the valence spinors are classified according to the O_h^* double group symmetry and all the t groups undergo a spin-orbit splitting into an f and e spinor accommodating four and two electrons, respectively. In detail, we have the following correlation between the O_h and O_h^* ireps: $a_{1g}\rightarrow e_{1g}$, $e_g\rightarrow f_g$, $t_{(1,2)(g,u)}\rightarrow f_{(g,u)}+e_{(1,2),(g,u)}$. The nuclear charges of the constituent atoms do not cause strong scalar relativistic and spin-orbit effects which leads to a clear separation of the individual t group components appearing as pairs of closely spaced doublets which may not be resolvable in an experimental PE spectrum. In the following we summarize the characteristics in the SiF_6^{2-} spectrum. It should be kept in mind that speaking of an ionization from a specific Hartree-Fock orbital $|\varphi_p\rangle$ is correct up to zeroth order only because electron correlation is implicitly accounted for in the ADC scheme.The *exact* $N-1$-particle state $|\Psi_n^{N-1}\rangle$ can formally be written as a linear combination of so-called *intermediate states* $|\tilde{\Psi}_I\rangle$ bearing electron correlation according to their construction principle [69–71],

$$|\Psi_n^{N-1}\rangle = \sum_I X_{In}|\tilde{\Psi}_I\rangle = \sum_q X_{qn}|\tilde{\Psi}_q\rangle + \cdots . \tag{8}$$

Hereby I labels the excitation classes ($1h$, $2h1p$, $3h2p$, …) and q refers to the $1h$ states explicitly. As can be seen from Fig. 2 and Table I the pole strengths of all SiF_6^{2-} peaks under consideration are 92% reflecting a pronounced main state character of the various monoanionic final states. Therefore the one-particle picture of photoionization is a good approximation [49] where this picture is hereby to be understood in

TABLE I. Comparison of the correlated and Koopmans SiF_6^{2-} ionization energies (in eV). The nonrelativistic unsplit parent state is given in parentheses after the symbol for the relativistic final state. Additionally, the pole strengths and populations of the corresponding DHF spinors are given. Contributions below 1% are not listed.

Final state	DHF-ADC(3)	Koopmans	Pole strength	Population
$3F_g(\pi T_{1g})$	2.789	4.775	0.92	97% Fp
$2E_{1g}(\pi T_{1g})$	2.826	4.816	0.92	97% Fp
$3F_u(\pi T_{1u})$	3.659	5.507	0.92	94% Fp
$2E_{1u}(\pi T_{1u})$	3.727	5.586	0.92	95% Fp
$1E_{2u}(\pi T_{2u})$	3.738	5.693	0.92	99% Fp
$2F_u(\pi T_{2u})$	3.771	5.730	0.92	99% Fp
$2F_g(\sigma E_g)$	4.545	6.225	0.92	98% Fp
$1E_{2g}(\pi T_{2g})$	5.569	7.451	0.92	99% Fp
$1F_g(\pi T_{2g})$	5.597	7.484	0.92	99% Fp
$1E_{1u}(\sigma T_{1u})$	6.877	8.586	0.92	81%Fp,16% Sip
$1F_u(\sigma T_{1u})$	6.892	8.607	0.92	78%Fp,16% Sip
$1E_{1g}(\sigma A_{1g})$	9.317	10.94	0.92	81%Fp, 6% Fs,12% Sis

a quasiparticle sense. A main state in the expansion (8) would therefore be represented by one dominant intermediate state $|\tilde{\Psi}_p\rangle$ with $X_{pn}\approx 1$ and the other $X_{qn}\approx 0$ for $q\neq p$. Again, an actual expansion of the dominant intermediate state starts with the corresponding $1h$ Slater determinant in zeroth order where the orbital $|\varphi_p\rangle$ is annihilated. The $1h$ final states are classified according to the symmetry of this $1h$ state. If the leading $1h$ configuration of a final state would be, for example, $[\text{core}]3f_g^{-1}$, the corresponding state is denoted as $3F_g$ in Table I. Together with a pronounced main state character substantial deviations of the ionization potentials with respect to the Koopmans energies can be observed (see Table I) reflecting the importance of correlation contributions to the $1h$ final states. Additionally, the resulting monoanionic states do not exhibit satellite structure which means that they are not degenerate with other $2h1p$ configurations where an additional electron is excited from an occupied to a virtual orbital. This degeneracy is much more likely for subvalence and inner valence orbitals and the originally acquired pole strength is then distributed over many $2h1p$ configurations (satellites). In the SiF_6^{2-} spectrum no satellites with notable intensity could be observed in the energy range between 9.3 eV and 21 eV.

From the populations in Table I it is clearly visible that the first nine ionizations lead to final states possessing pure ligand character. The orbitals of the central atom come into play when the ionization starts to occur from subvalence orbitals resulting in the $1E_{1u}$, $1F_u$, and $1E_{1g}$ final states. Spin-orbit coupling only leads to small splits of the t groups not causing any level interlacing and is therefore of minor importance for the overall spectral structure. Especially by the absence of occupied central atom d orbitals which normally exhibit a considerable participation in the valence region the spectrum is largely dominated by the character of the ligand atoms. An example for a dianionic hexafluoro complex with strong metal-d contributions to the valence spinors is PtF_6^{2-} [34]. In a scalar relativistic description the highest occupied molecular orbital (HOMO) of the latter complex is formed by the $2t_{2g}$ orbital consisting of Pt d and F $p(\pi)$ in equal parts indicating a considerable Pt $d(t_{2g})$/F $2p$ interaction. Even in the presence of six fluorine ligands with nonbonding $2p$ orbitals the platinum d functions contribute considerably to the valence ionized final states. Additionally, the full DHF-ADC(3) description of PtF_6^{2-} yields a spin-orbit splitting of the outer $2t_{2g}$ orbital in a $2e_{2g}$ and $4f_g$ spinor separated by 0.82 eV now essentially influencing the spectral structure. This is characteristic for d orbitals which are very sensitive to electron correlation effects and exhibit considerable spin-orbit splitting in heavy systems.

The theoretical findings reveal a considerable stability against electron autodetachment of the SiF_6^{2-} complex which is reflected in the first ionization potential of 2.79 eV. In this respect SiF_6^{2-} is more stable than the transition metal homologues CrF_6^{2-}, PtF_6^{2-}, and MoF_6^{2-} [2] where a metal d orbital participation in the valence final states is realized. For a more elaborate investigation the lifetime of SiF_6^{2-} and the rate of dissociation into $SiF_5^-+F^-$should be calculated. By application of the local spin-density approximation Gutsev obtained an instability of SiF_6^{2-} towards dissociation which amounts to −1.90 eV [72]. Taking the dissociative character of SiF_6^{2-} into account he additionally determined the adiabatic electron affinity of SiF_6^- as 2.58 eV, which would correspond to the ionization energy of SiF_6^{2-}. However, one cannot directly compare these values due to various aspects. At first, we always calculate vertical ionization potentials starting from the minimum geometry of SiF_6^{2-} and for the shifted equilibrium distance of the monoanion this will lead to noticeable differences in the vertical and adiabatic ionization potentials (IPs). Secondly, the applied computational methods are based on different grounds further hampering a straightforward comparison. Detailed calculations employing size-consistent correlation methods and a correction for the basis set superposition error are therefore requested for an accurate determination of the SiF_6^{2-} dissociation channel which is not part of the current investigation.

SiF_6^{2-} is isoelectronic to SF_6 which exhibits a considerable stability and similar mechanisms as in SF_6 may stabilize

the SiF_6^{2-} dianion as well. Especially the role of *d* orbitals, covalency and hybridization for SF_6 as a hypervalent species was intensively discussed in the literature (see, for example, [73] and references therein). For SF_6 it was hereby found that the sulfur *d* orbitals have a pronounced effect on the total energy of the system [73] despite their low electron occupancy which excludes a sp^3d^2 hybridization model. A Mulliken population analysis of the SiF_6^{2-} valence spinors also yields only negligible Si *d* contributions, but this kind of analysis is not best suited for the study of the bonding situation in compounds with strongly ionic character [74,75]. For a detailed analysis one should therefore resort to a natural population and natural hybrid orbital analysis. Then a comparative consideration of the bonding situation in SF_6 and SiF_6 may lead to further insight and studies in this direction are underway.

V. CONCLUSIONS

The existence of the dianion SiF_6^{2-}, produced by sputtering, has been verified by accelerator mass spectrometry. The dianion's flight time through the mass spectrometer of about 20 μs constitutes a lower limit in terms of its lifetime. A theoretical calculation of the corresponding photoelectron spectrum using the method of the four-component one-particle propagator reveals typical main group characteristics in the spectrum and predicts considerable stability against autodetachment. Spin-orbit coupling has only a minor influence on the overall spectral features and no silicon *d* orbital participation was found in the outer valence final states. For a decisive theoretical statement about the SiF_6^{2-} lifetime the dissociation probability into SiF_5^- and F^- should also be calculated but these demanding computations were not part of the theoretical framework which primarily focused on the valence ionization spectrum and stability against electron detachment.

ACKNOWLEDGMENTS

Two of the authors (H.G. and M.P.) gratefully acknowledge financial support by the Deutsche Forschungsgemeinschaft.

[1] J. Kalcher and A. F. Sax, Chem. Rev. (Washington, D.C.) **94**, 2291 (1994).
[2] M. K. Scheller, R. N. Compton, and L. S. Cederbaum, Science **270**, 1160 (1995).
[3] A. I. Boldyrev, M. Gutowski, and J. Simons, Acc. Chem. Res. **29**, 497 (1996).
[4] G. Freeman and N. March, J. Phys. Chem. **100**, 4331 (1996).
[5] L. S. Wang and X. B. Wang, J. Phys. Chem. A **104**, 1978 (2000).
[6] A. Dreuw and L. S. Cederbaum, Chem. Rev. (Washington, D.C.) **102**, 181 (2002).
[7] D. Mathur, Phys. Rep. **391**, 1 (2003).
[8] S. N. Schauer, P. Williams, and R. N. Compton, Phys. Rev. Lett. **65**, 625 (1990).
[9] H. Gnaser and H. Oechsner, Nucl. Instrum. Methods Phys. Res. B **82**, 518 (1993).
[10] R. Middleton and J. Klein, Nucl. Instrum. Methods Phys. Res. B **123**, 532 (1997).
[11] H. Gnaser, Nucl. Instrum. Methods Phys. Res. B **149**, 38 (1999).
[12] H. Gnaser and R. Golser, Chem. Phys. **329**, 222 (2006).
[13] X. B. Wang and L. S. Wang, J. Chem. Phys. **111**, 4497 (1999).
[14] X. B. Wang and L. S. Wang, Phys. Rev. Lett. **83**, 3402 (1999).
[15] J. Friedrich, P. Weis, J. Kaller, R. L. Whetten, and M. M. Kappes, Eur. Phys. J. D **9**, 269 (1999).
[16] L. S. Wang and X. B. Wang, J. Am. Chem. Soc. **122**, 2339 (2000).
[17] P. Weis, O. Hampe, S. Gilb, and M. M. Kappes, Chem. Phys. Lett. **321**, 426 (2000).
[18] M. Blom, O. Hampe, S. Gilb, P. Weis, and M. M. Kappes, J. Chem. Phys. **115**, 3690 (2001).
[19] J. Friedrich, S. Gilb, O. Ehrler, A. Behrendt, and M. M. Kappes, J. Chem. Phys. **117**, 2635 (2002).
[20] A. Dreuw and L. S. Cederbaum, Phys. Rev. A **63**, 012501 (2000).
[21] R. Middleton and J. Klein, Phys. Rev. A **60**, 3515 (1999).
[22] R. Golser, H. Gnaser, W. Kutschera, A. Priller, P. Steier, C. Vockenhuber, and A. Wallner, Nucl. Instrum. Methods Phys. Res. B **240**, 468 (2005).
[23] H. Gnaser, Nucl. Instrum. Methods Phys. Res. B **197**, 468 (2002).
[24] K. Franzreb and P. Williams, J. Chem. Phys. **123**, 224312 (2005).
[25] X.-L. Zhao and A. E. Litherland, Phys. Rev. A **71**, 064501 (2005).
[26] R. Golser, H. Gnaser, W. Kutschera, A. Priller, P. Steier, and A. Wallner, Nucl. Instrum. Methods Phys. Res. B **259**, 71 (2007).
[27] M. K. Scheller and L. S. Cederbaum, J. Phys. B **25**, 2257 (1992).
[28] M. K. Scheller and L. S. Cederbaum, Chem. Phys. Lett. **216**, 141 (1993).
[29] M. K. Scheller and L. S. Cederbaum, J. Chem. Phys. **99**, 441 (1993).
[30] T. Sommerfeld and M. S. Child, J. Chem. Phys. **110**, 5670 (1999).
[31] H.-G. Weikert, L. S. Cederbaum, F. Tarantelli, and A. I. Boldyrev, Z. Phys. D: At., Mol. Clusters **18**, 7122 (1991).
[32] H.-G. Weikert and L. S. Cederbaum, J. Chem. Phys. **99**, 8877 (1993).
[33] T. Sommerfeld, S. Feuerbacher, M. Pernpointner, and L. S. Cederbaum, J. Chem. Phys. **118**, 1747 (2003).
[34] M. Pernpointner and L. S. Cederbaum, J. Chem. Phys. **126**, 144310 (2007).
[35] J. Schirmer, L. S. Cederbaum, and O. Walter, Phys. Rev. A **28**, 1237 (1983).
[36] M. Pernpointner, J. Breidbach, and L. S. Cederbaum, J. Chem. Phys. **122**, 064311 (2005).

[37] M. Pernpointner and A. B. Trofimov, J. Chem. Phys. **120**, 4098 (2004).
[38] M. Pernpointner, J. Chem. Phys. **121**, 8782 (2004).
[39] DIRAC, a relativistic *ab initio* electronic structure program, Release DIRAC04.0 (2004), written by H. J. Aa. Jensen, T. Saue, and L. Visscher with contributions from V. Bakken, E. Eliav, T. Enevoldsen, T. Fleig, O. Fossgaard, T. Helgaker, J. Laerdahl, C. V. Larsen, P. Norman, J. Olsen, M. Pernpointner, J. K. Pedersen, K. Ruud, P. Salek, J. N. P. van Stralen, J. Thyssen, O. Visser, and T. Winther (http://dirac.chem.sdu.dk).
[40] RELADC Version 0.9.0 (2004) and Version 1.0.0 (2006): program for the fully relativistic calculation of the one-particle propagator using the ADC(3) approach, written by M. Pernpointner.
[41] C. Vockenhuber, I. Ahmad, R. Golser, W. Kutschera, V. Liechtenstein, A. Priller, P. Steier, and S. Winkler, Int. J. Mass. Spectrom. **223**, 713 (2003).
[42] P. Steier, R. Golser, W. Kutschera, A. Priller, C. Vockenhuber, and S. Winkler, Nucl. Instrum. Methods Phys. Res. B **223-224**, 67 (2004).
[43] H. Migeon, C. L. Pipec, and J. L. Goux, in *Secondary Ion Mass Spectrometry SIMS V*, edited by A. Benninghoven *et al.* (Springer, Berlin, 1986), p. 155.
[44] A. A. Abrikosov, L. P. Gorkov, and I. E. Dzyaloshinski, *Methods of Quantum Field Theory in Statistical Physics* (Prentice-Hall, Englewood Cliffs, NJ, 1963).
[45] A. L. Fetter and J. D. Walecka, *Quantum Theory of Many-Particle Systems* (McGraw-Hill, New York, 1971).
[46] R. D. Mattuck, *A Guide to Feynman Diagrams in the Many-Body Problem* (McGraw-Hill, New York, 1967).
[47] L. S. Cederbaum and W. Domcke, Adv. Chem. Phys. **36**, 205 (1977).
[48] J. Simons, Annu. Rev. Phys. Chem. **28**, 1 (1977).
[49] L. S. Cederbaum, W. Domcke, J. Schirmer, and W. von Niessen, Adv. Chem. Phys. **65**, 115 (1986).
[50] J. Oddershede, Adv. Quantum Chem. **11**, 275 (1978).
[51] M. F. Herman, K. F. Freed, and D. L. Yeager, Adv. Chem. Phys. **48**, 1 (1981).
[52] Y. Öhrn and G. Born, Adv. Quantum Chem. **13**, 1 (1981).
[53] W. von Niessen, J. Schirmer, and L. S. Cederbaum, Comput. Phys. Rep. **1**, 57 (1984).
[54] J. V. Ortiz, J. Chem. Phys. **104**, 7599 (1996).
[55] J. V. Ortiz, J. Chem. Phys. **108**, 1008 (1998).
[56] J. Schirmer, Phys. Rev. A **26**, 2395 (1982).
[57] I. P. Grant and H. M. Quiney, Adv. At. Mol. Phys. **23**, 37 (1988).
[58] H. M. Quiney, Methods Comput. Chem. **2**, 223 (1988).
[59] H. M. Quiney, I. P. Grant, and S. Wilson, Phys. Scr. **36**, 460 (1987).
[60] H. M. Quiney, I. P. Grant, and S. Wilson, *Many-body Methods in Quantum Chemistry*, edited by U. Kaldor (Springer, Berlin, 1989).
[61] S. Wilson, *The Effects of Relativity on Atoms, Molecules and the Solid State* (Plenum Press, New York, 1991).
[62] J. Schirmer and G. Angonoa, J. Chem. Phys. **91**, 1754 (1989).
[63] W. C. Hamilton, Acta Crystallogr. **15**, 353 (1962).
[64] M. L. Yu, in *Sputtering by Particle Bombardment III*, edited by R. Behrisch and K. Wittmaack (Springer, Berlin, 1991), p. 91.
[65] H. Gnaser, *Low-Energy Ion Irradiation of Solid Surfaces* (Springer, Berlin, 1999).
[66] H. Gnaser, Phys. Rev. B **54**, 16456 (1996).
[67] H. Gnaser, Phys. Rev. B **63**, 045415 (2001).
[68] R. Golser, H. Gnaser, W. Kutschera, A. Priller, P. Steier, and C. Vockenhuber, Nucl. Instrum. Methods Phys. Res. B **223-224**, 221 (2004).
[69] J. Schirmer, Phys. Rev. A **43**, 4647 (1991).
[70] F. Mertins and J. Schirmer, Phys. Rev. A **53**, 2140 (1996).
[71] J. Schirmer and F. Mertins, Int. J. Quantum Chem. **58**, 329 (1996).
[72] G. L. Gutsev, Chem. Phys. Lett. **184**, 305 (1991).
[73] A. E. Reed and F. Weinhold, J. Am. Chem. Soc. **108**, 3586 (1986).
[74] A. E. Reed, R. B. Weinstock, and F. Weinhold, J. Chem. Phys. **83**, 735 (1985).
[75] J. Collins and A. Streitwieser, J. Comput. Chem. **1**, 81 (1980).